

Dup

# SEARCH FOR MAGNETIC DIPOLE STRENGTH AND GIANT SPIN-FLIP

## RESONANCES IN HEAVY NUCLEI

D. J. HOREN

Oak Ridge National Laboratory,  
Oak Ridge, Tennessee 37830 USA

### ABSTRACT

A description is given of the use of high resolution (n,n) scattering and the (p,n) reaction as tools to investigate highly excited states with emphasis on information pertaining to magnetic dipole strength and giant spin-flip resonances in heavy nuclei. It is shown how the ability to uniquely determine the spins and parities of resonances observed in neutron scattering has been instrumental to an understanding of the distribution of M1 strength in  $^{207,208}\text{Pb}$ . Some recent results of (p,n) studies with intermediate energy protons are discussed. Energy systematics of the giant Gamow-Teller (GT) resonance as well as a new  $\Delta L = 1$ ,  $\Delta S = 1$  resonance with  $J^\pi = (1,2)^-$  are presented. It is shown how the (p,n) reaction might be useful to locate M1 strength in heavy nuclei.

### 1. INTRODUCTION

Although a good deal of effort has been expended in investigations of the nuclear continuum regions of excitation, there still are many features which are not yet understood as well as others which have not yet been observed. Researchers have utilized many different techniques in their pursuit of these problems, and in recent years we have witnessed the demise of some of these methods and the introduction of new ones. This work will concentrate on just two methods: 1) high resolution low-energy neutron scattering ("old" technique) and 2) high energy (p,n) reaction studies ("new"

technique). The main emphasis will be upon aspects of the data and physics, rather than the experimental details. The neutron scattering measurements provide a microscopic view of an energy window which commences at the neutron separation energy and can extend up to as much as a few MeV for some targets. It will become clear that such microscopic detail can be of crucial importance for obtaining a proper description of some aspects of the nuclear continuum.

## 2. THE (n,n) REACTION

Although much information has been derived from the study of low energy neutron induced reactions, the recent availability of facilities<sup>1)</sup> which provide high intensities as well as high resolution has opened a whole new vista of possibilities. The first figure summarizes some of the quantities

ORNL WS-10249

### HIGH RESOLUTION NEUTRON EXPERIMENTS

#### QUANTITIES MEASURED

- RESONANCE PARAMETERS ( $E_r$ ,  $J^\pi$ ,  $\Gamma_n$ ,  $\Gamma_\gamma$ , etc.)
- POTENTIAL PHASE SHIFTS

#### PROPERTIES DEDUCED

- NEUTRON STRENGTH FUNCTIONS
- DOORWAY STATES
- NUCLEAR LEVEL DENSITIES
- ELECTROMAGNETIC RADIATIVE STRENGTH  
( $E1$ ,  $M1$ ,  $E2$ )
- OPTICAL MODEL PARAMETERS

Fig. 1. Some uses of high resolution neutron measurements. that can be determined from high resolution neutron measurements. These include resonance energies ( $E_r$ ), spins and parities ( $J^\pi$ ) neutron widths ( $\Gamma_n$ ), radiative widths ( $\Gamma_\gamma$ ), non-resonance phase shifts, etc. From these

measured quantities it is possible to deduce information pertaining to 1) neutron strength functions, 2) intermediate structure, 3) electromagnetic radiative strengths, 4) nuclear level densities and 5) optical model parameters. Although each of these topics has been around for a rather long period, the availability of quantitative data to examine them has been somewhat lacking. Furthermore, as we shall see, most of these are still of current theoretical interest. This point will be examined by looking at the results of some recent high resolution neutron transmission and differential elastic scattering measurements performed at the Oak Ridge Electron Linear Accelerator (ORELA). The only experimental details that will be given here are that the electron burst width was approximately 5 ns and the neutron flight path was 200 meters.

Figure 2 shows some typical total and differential elastic scattering data<sup>2)</sup> for a target of  $^{206}\text{Pb}$ . The data were analyzed using computer codes<sup>3)4)5)</sup> based upon R-matrix theory.<sup>6)7)</sup> For resonances which have neutron widths comparable to or greater than the experimental resolution, resonance parameters can be determined with confidence. The peak cross section is sensitive to the resonance spin, and the shape is a signature of the angular momentum transfer. The resonance at 146 keV is clearly an s-wave because of its large interference pattern in the total cross section spectrum. Examples of p- and d-waves are also indicated in

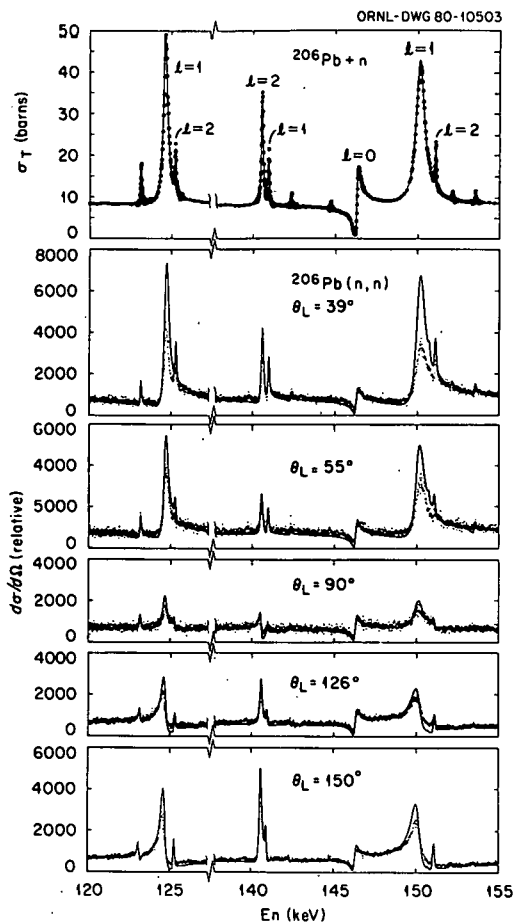


Fig. 2. Total and differential elastic cross sections for  $^{206}\text{Pb} + n$  for  $E_n = 120\text{--}155$  keV (from reference 2).

the figure. As can be seen, there is a clear distinction between the behavior of the shapes of resonances which involve s-, p- or d-waves. Higher angular momentum transfers need not be considered at these energies, as their penetrabilities are relatively small. Note that at ~125 keV there is a closely lying doublet (p- and d-wave) as well as at ~140 keV (d- and p-wave). From these data, it has been clearly shown<sup>2)</sup> that most of the radiative strength at these energies consists of E1 radiation rather than M1 which had been reported<sup>8)</sup> from a ( $\gamma$ ,n) study at poorer resolution. The solid curve in the total cross section spectrum is a result of a least squares fit to the data. The solid curves in the differential scattering spectra are calculations using the parameters determined from that fit. To date, the data have been analyzed up to a neutron energy of ~900 keV with comparable results, and parameters have been determined for approximately 400 resonances.

#### Doorway States

In Fig. 3 is shown a plot of the sum of the reduced neutron widths for

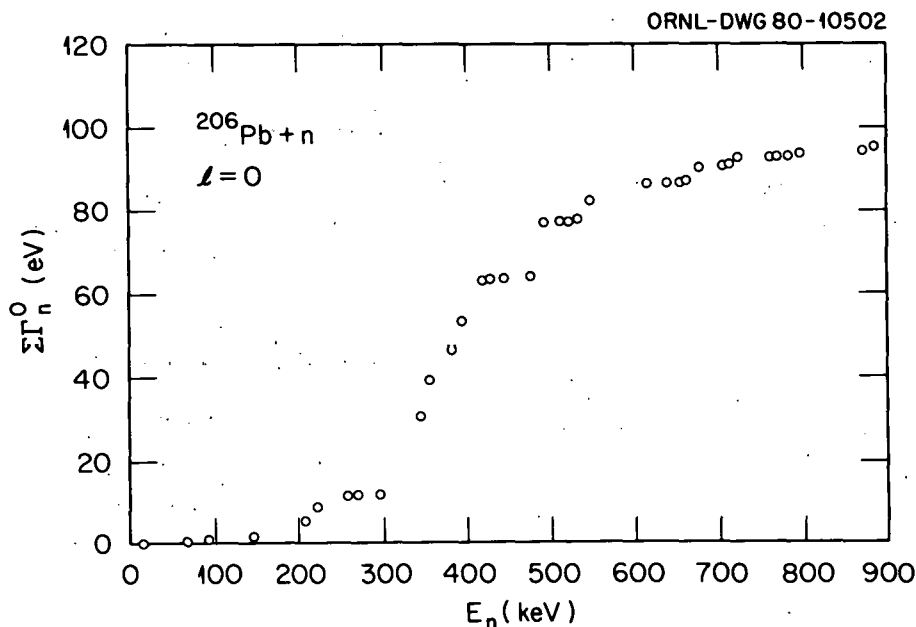


Fig. 3. Plot of the sum of the reduced neutron widths for s-wave resonances versus neutron energy.

s-waves versus neutron energy. The strength function is given by the slope of the curve. The change in the s-wave strength function in the vicinity of 400 keV (which is common to a number of lead isotopes) was first reported by Farrell et al.<sup>9)</sup> and suggested as a common doorway state which has been described<sup>10)</sup> in terms of a  $(2g_{9/2}, 4^+)$  particle-core excitation by Beres and Divadeenam. Similar plots for the p-wave and d-wave strength functions are shown in Figs. 4 and 5

respectively. Doorway states are seen to occur at widths for p-waves versus neutron energy (from ~40 keV in the  $p_{1/2}$  channel and ~145 keV in the  $p_{3/2}$  channel. The summed strength in these p-wave doorway states is comparable to that found for analogous doorway states observed<sup>11)</sup> in the  $^{207}\text{Pb} + n$  reaction. These doorway states have been suggested<sup>2)</sup> to arise from a  $(3d_{5/2}, 3^-)$  particle-core excitation. Most of the  $3d_{5/2}$  single-particle strength in  $^{207}\text{Pb}$  is known<sup>12)</sup> to be concentrated within a few levels located near 4.39 MeV. As can be seen from Fig. 6, the p-wave doorways occur at an excitation energy that is within about 200 keV of the sum of the energies of the  $3d_{5/2}$  strength (4.39 MeV) and  $3^-$  core excitation (2.65 MeV). Furthermore, the ratio of the strengths within the doorways agrees very well with the square of the ratio of the respective 3-j symbols  $\left(\begin{smallmatrix} 3 & 5/2 & j \\ 0 & -1/2 & 1/2 \end{smallmatrix}\right)$ . Separate plots of the  $d_{3/2}$  and  $d_{5/2}$  reduced widths show a concentration of

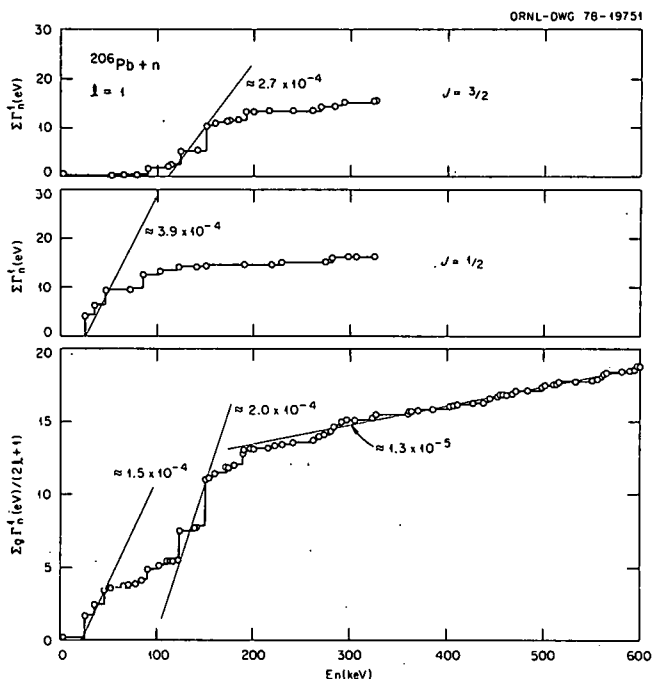


Fig. 4. Plots of the sum of reduced neutron widths for p-waves versus neutron energy (from reference 2).

strength in the vicinity of  $E_n = 350-400$  keV. These doorway states have been interpreted as also being due to the  $(2g_{9/2}, 4^+)$  particle-core coupling which can give rise to levels with spins ranging from  $J = 1/2 - 17/2$ . It might be recalled that the basis of the "doorway state" formalisms<sup>13)</sup> dates back to the early 1960's. Even with the abundance of neutron data generated thus far, the number of cases for which doorway states have been observed in neutron scattering is rather meager.

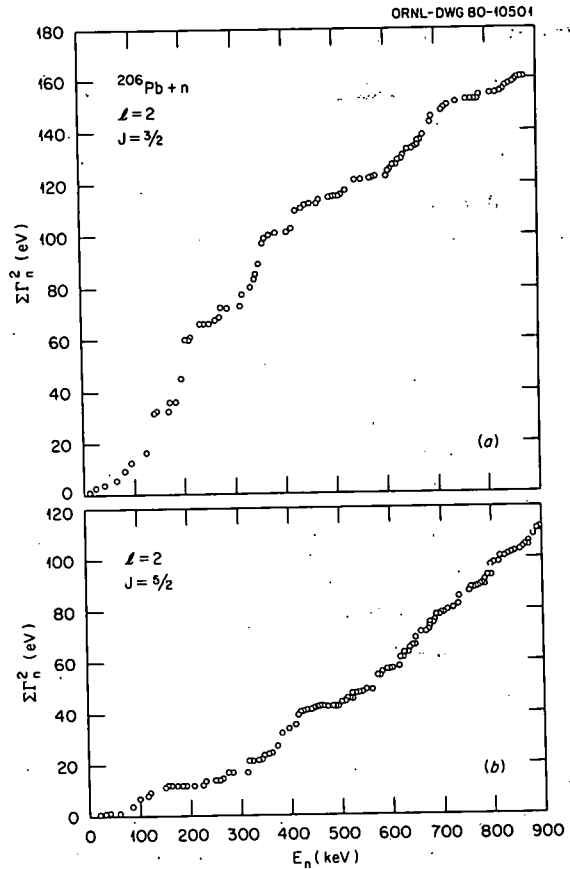


Fig. 5. Plots of the sum of reduced neutron widths for d-waves versus neutron energy.

The importance of observing and understanding particle-core excitations that lie in the nuclear continuum is still an open question. We note that for  $^{207,208}\text{Pb}$  the  $(3d_{5/2}, 3^-)$  particle-core excitation can lead to levels with the same  $J^\pi$  which is involved in M1 transitions, and the excitation energy lies within 1-2 MeV of the  $i_{11/2}^{-1} i_{13/2}^{-1}$  particle-hole excitation.

#### M1 Strength in $^{207,208}\text{Pb}$

As already noted above, the high resolution which can be achieved at ORELA has proved instrumental in helping to clarify the question of M1 strength in  $^{207,208}\text{Pb}$ . During the past few years this work has shown<sup>11)14)15)</sup> that many of the resonances in  $^{207}\text{Pb} + n$  that had been

reported to have large M1 radiation widths have in fact  $J^\pi = 1^-$ . Concurrently, photoneutron polarization measurements<sup>16)17)</sup> were doing likewise. Brief summaries of the demise of most of the purported M1 strength in  $^{208}\text{Pb}$  can be found in references 18) and 19). Only the status of a level near 8.0 MeV ( $E_n \approx 616$  keV) which had been reported<sup>16)</sup> to have a large M1 radiation width will be discussed here.

Total and differential elastic scattering cross sections for  $E_n = 600-625$  keV are shown<sup>15)</sup> in Fig. 7 where eleven resonances are identified. Resonances with large d-wave

neutron width are confidently assigned on the basis of their interference minima at  $90^\circ$  and enhanced peak cross sections at  $150^\circ$ . R-matrix fits to the data showed the 606-keV resonance to be an s- and d-wave admixture, and the 616-keV resonance to be almost pure d-wave, both with  $J^\pi = 1^-$ . Only two peaks were observed in the  $(\gamma, n)$  reaction in the same energy interval. The resonance at 606 keV was properly identified as  $1^-$ , while a 616-keV resonance was assigned as  $1^+$  based upon the interference observed in photoneutron polarization measurements<sup>16)</sup>. However, when the results of the high resolution neutron measurements were combined with the photoneutron angular distribu-

ORNL - DWG 80-10500

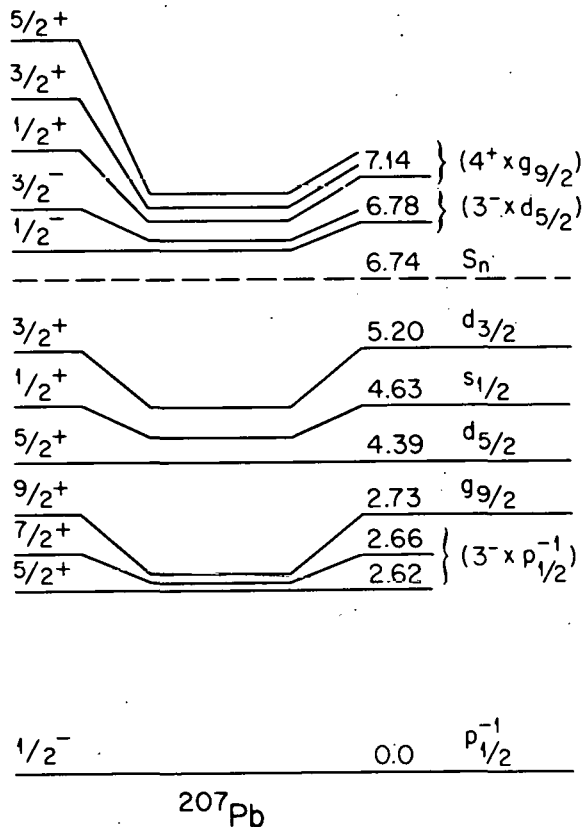


Fig. 6. Partial energy level diagram for  $^{207}\text{Pb}$ .

tion<sup>20)</sup> and polarization<sup>16)</sup> data, it was found<sup>15)</sup> that little if any M1 radiation could be present in the vicinity of the 616-keV resonance. Furthermore, it was observed that the photoneutron data could be fit almost as well by assuming a nearby resonance at 616.8 keV (shown to involve  $\ell = 1$ ) had  $J^\pi = 2^+$ ; i.e., E1 + E2 interference can lead to similar photoneutron polarizations as E1 + M1 interference. Historically, it was after such lengthy analysis was completed, that a  $(n, \gamma)$  measurement was made at ORELA using a neutron flight path of 150

meters. A comparison between the  $(n, n)$

and  $(n, \gamma)$  spectra for the energy interval 608–625 keV is shown in Fig. 8 where the energy correspondence of the resonances under discussion is clearly evident. Furthermore, this figure clearly confirms the above conclusions that the preponderance of ground-state radiation in the vicinity of 616 keV is associated with the  $1^-$  resonance.

The experimental status of M1 strength in the unbound region of  $^{208}\text{Pb}$  is as follows: Between 7.384 and 7.993 MeV there are approximately thirty-four

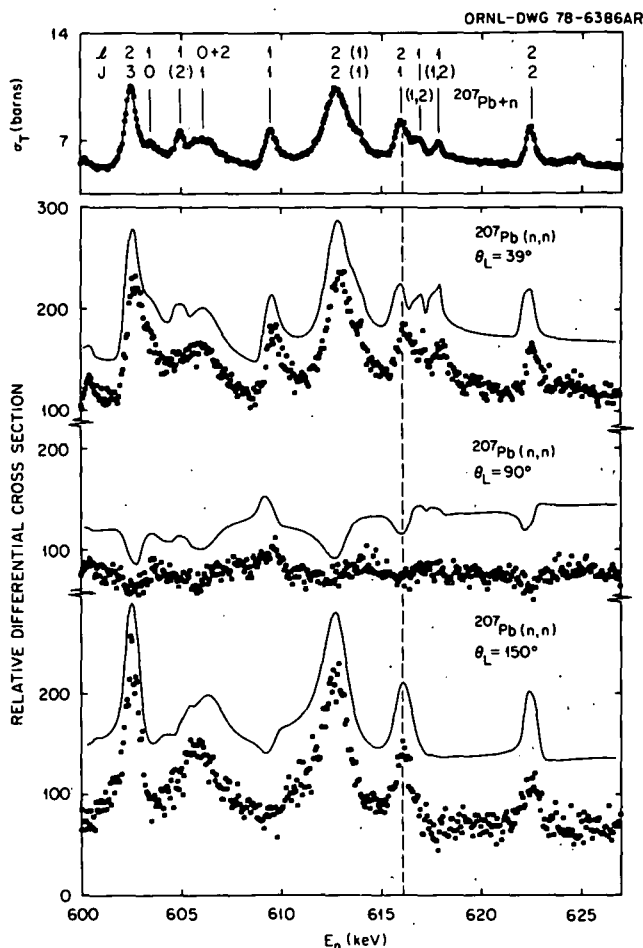


Fig. 7. Total and differential elastic scattering cross sections for  $^{207}\text{Pb} + n$  near  $E_n = 600$  keV.



1<sup>+</sup> resonances<sup>11)14)18)</sup> which have  $B(M1)_{+} = 2.6 \mu_0^2$ . Above 8.4 MeV, photoneutron polarization work<sup>21)</sup> has suggested additional M1 strength based upon the observation of neutron polarization at 90°. However, as noted above, E1-E2 interference can also give rise to such polarization, hence care must be exercised in drawing conclusions about the presence of M1 radiation from such measurements. In the bound-state region there is a state<sup>22)</sup> at 7.279 MeV with  $B(M1)_{+} = 0.17 \mu_0^2$ . Strength associated with a state at 4.83 MeV has recently been questioned.<sup>23)</sup>

The experimental situation in the unbound region of  $^{207}\text{Pb}$  is more difficult to ascertain. However, something can be said about a quantity which is proportional to the ground-state radiative strength, i.e.,  $(g_{\gamma} \Gamma_{\gamma} \Gamma_n)/\Gamma$ . This is shown in Fig. 9 where the solid histogram is from a  $(\gamma, n)$  study<sup>8)</sup> and the dashed histogram represents the modified values based upon the ORELA  $(n, n)$  measurements. It would be desirable to have higher quality photon data for  $^{207}\text{Pb}$  so as to be able to determine absolute strengths and to make a comparison to M1 strength in  $^{208}\text{Pb}$ .

#### Nuclear Level Densities in $^{207}\text{Pb}$

Before leaving the topic of  $(n, n)$  measurements, a few words will be

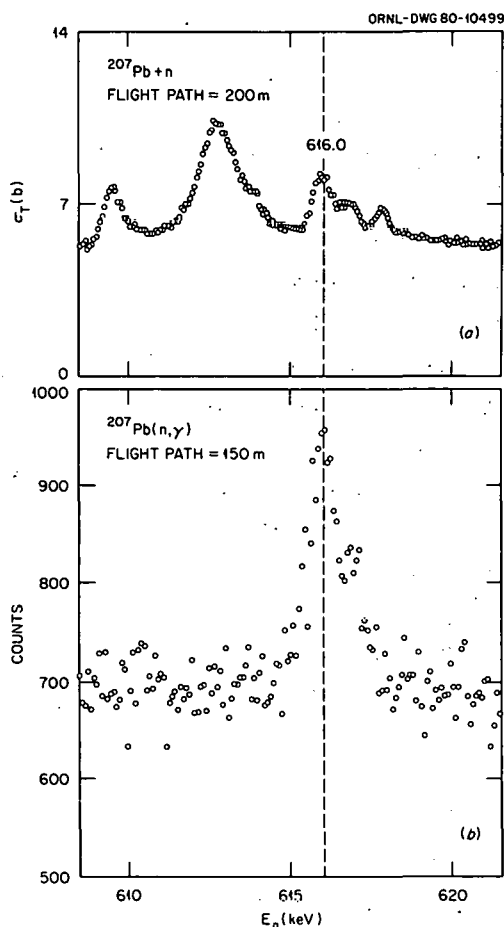


Fig. 8. Comparison of  $^{207}\text{Pb} + n$  and  $^{207}\text{Pb}(n, \gamma)$  in the vicinity of the 616 keV resonance. (From unpublished work at ORELA.)

devoted to another old topic, i.e., nuclear level densities whose knowledge is important for an understanding of spreading widths of giant resonances.

Although it is usually assumed that nuclear level densities can be expressed<sup>24)</sup> in terms of a relation which has a  $(2J+1)$  dependence and is independent of parity, quantitative data with which to test these hypotheses is somewhat lacking. The sum of the s-, p- and d-wave resonances, respectively, for  $^{206}\text{Pb} + n$  are plotted as a function of

neutron energy in Fig. 10. The s-wave data have been compared with a constant temperature model where the density of levels with given  $J^\pi$  was taken as

$$\rho(E_x, J^\pi) = (J + 1/2) k e^{E_x/T},$$

where  $E_x = S_n + E$ , the neutron separation and kinetic energy, respectively, and  $k$  and  $T$  are constants. Values of  $k$  and  $T$  were determined from fits (dashed curve) to the s-wave data. These were then used to calculate the

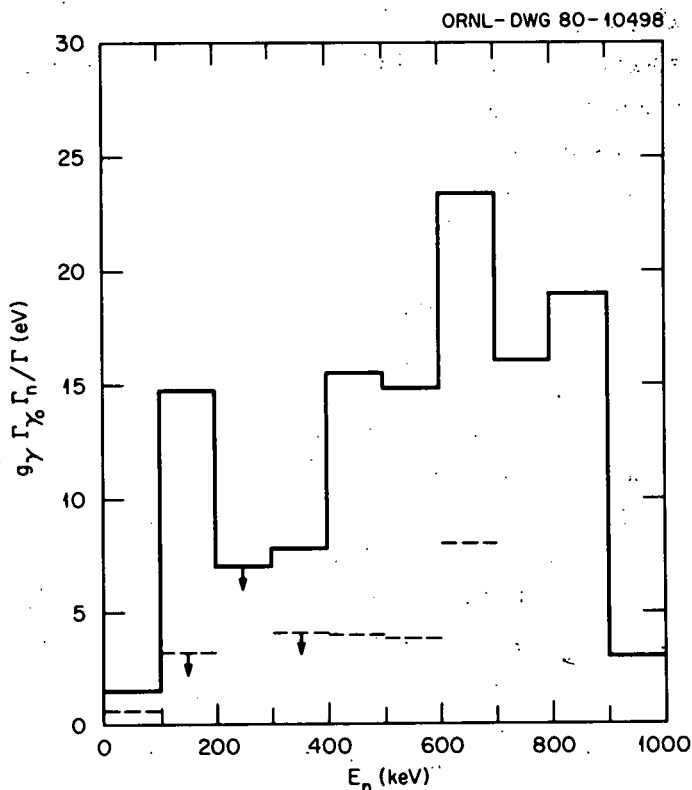


Fig. 9. Relative M1 strength from  $^{207}\text{Pb}(\gamma, n)$  reaction (solid histogram as modified by  $^{207}\text{Pb} + n$  work (dashed histogram)).

number of p- and d-wave resonances, respectively, and the results are shown as the dashed curves in Fig. 10. The fairly good agreement between the calculated and experimental curves for the d-waves is interpreted as an indication of the  $(2J+1)$  dependence of the level density formula. The overabundance of observed p-waves is interpreted as implying a parity dependence. Efforts are being made to determine whether or not shell model calculations can reproduce the observed level densities.

### 3. The (p,n) Reaction at Intermediate Energies

The availability of the beam swinger<sup>25)</sup> at the Indiana University Cyclotron Facility (IUCF) has provided a significant new tool for studying highly excited states. This section will be devoted to a discussion of recent work pertaining to the search for analogue resonances of M1 transitions and giant spinflip resonances.

It is interesting to note here also that the theoretical ground work was already initiated in the early 1960's. (One could even argue 1939.<sup>26)</sup>). Kawai et al.<sup>27)</sup> explored the effects of the spin-isospin interaction for the inelastic scattering of high energy protons, and Ikeda and coworkers<sup>28)</sup> postulated the existence of a giant Gamow-Teller (GT) resonance and pointed

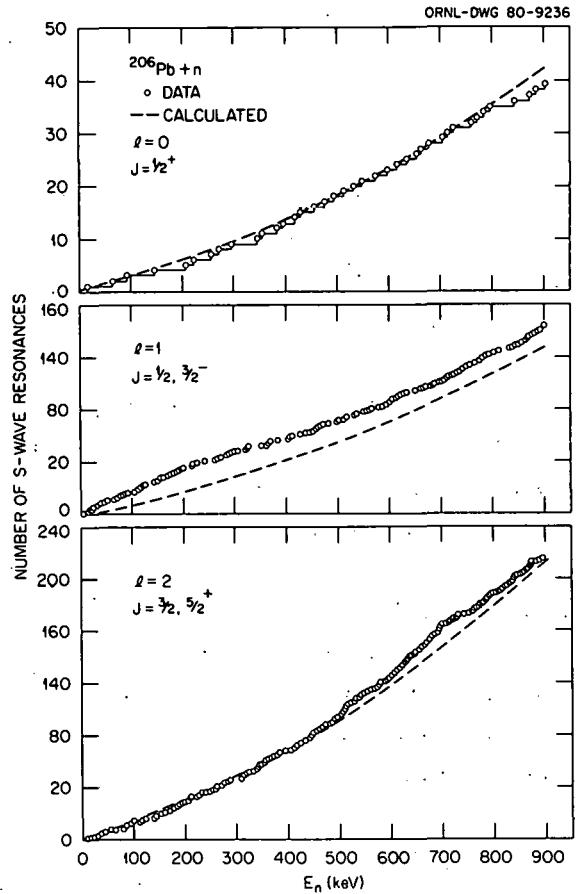


Fig. 10. Plots of the cumulative number of s-, p- and d-wave resonances (top to bottom, respectively) versus neutron energy for  $^{206}\text{Pb} + n$  reaction. The dashed lines represent calculated curves using a constant temperature model for the level densities.

out its accessibility via the (p,n) reaction.

The states expected to be excited in the (p,n) reaction by  $\Delta l = 0$  transitions are schematically illustrated in Fig. 11 where the dashed lines connect isobaric analogue states. Also shown are the M1 states in the target nucleus. The M1 operator can be expressed as the sum of two terms, one of which is isospin independent (isoscalar) and the other isospin dependent (isovector). The isoscalar component is proportional to

$$(M1)_{\text{isos}} \approx \mu_0 \times$$

$$\sum_i [1/2 \mu_+ \sigma_i + 1/2 \ell_i],$$

and the isovector part to

$$(M1)_{\text{isov}} \approx \mu_0 \sum_i \tau_3 [1/2 \mu_- \sigma_i - 1/2 \ell_i],$$

where  $1/2 \mu_+ = 0.44 \text{ nm}$  and  $1/2 \mu_- = -2.35 \text{ nm}$ , respectively. The isoscalar component can only give rise to transitions for which  $\Delta T = 0$ , whereas the isovector component can give rise to transitions for both  $\Delta T = 0, 1$ . Because  $\mu_-$  is considerably larger than  $\mu_+$ , isovector transitions are expected to dominate. The level labeled GT represents the giant GT-resonance predicted in reference 28). As seen in Fig. 11, the (p,n) reaction can cause

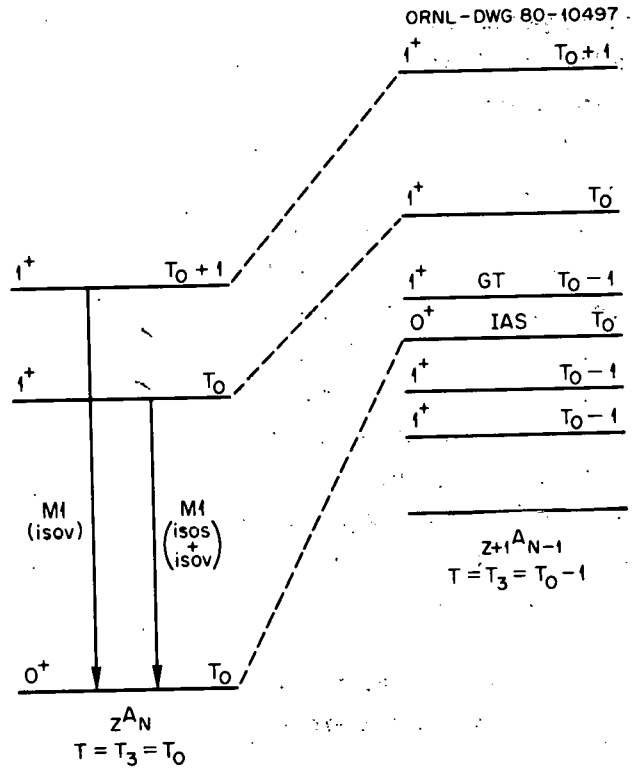


Fig. 11. Fermi and Gamow-Teller states that can be populated in the (p,n) reaction at small angles.

transitions to an isospin multiplet in the final nucleus when the isospin of the target (i.e.,  $T_0$ ) is nonzero. The relative cross sections to these states will be proportional to the squares of isospin Clebsch-Gordon coefficients. For the states with  $(T_0-1)$ ,  $T_0$  and  $(T_0+1)$  these are  $(2T_0-1)(2T_0+1)^{-1}$ ,  $(T_0+1)^{-1}$  and  $[(2T_0+1)(T_0+1)]^{-1}$ , respectively. Thus, for target nuclei with large  $T_0$ , one should mainly observe states in the final nucleus with isospin  $T=(T_0-1)$ .

Calculations of the (p,n) reaction in terms of the nucleon-nucleon (N-N) interaction at intermediate energies have been made by a number<sup>27)29)30)</sup> of authors. The isospin dependent part of the effective interaction is quite complicated and includes the following terms: central, spin-spin, spin-orbit and tensor-spin in all multipoles. However, for the distorted wave impulse approximation (DIA) in the limit of zero momentum transfer, only the  $\Delta l = 0$  terms survive and the contributions from spin-orbit and tensor-spin are unimportant.<sup>29)30)</sup> The zero degree cross sections can be expressed<sup>31)</sup> as

$$d\sigma/d\Omega(0^\circ) = (\mu/\pi\hbar^2)^2 k_f/k_i \{ N_T^D | J_T \langle F \rangle |^2 + N_{\sigma T} | J_{\sigma T} \langle GT \rangle |^2 \},$$

where  $\mu$  is the reduced mass,  $k_f$  and  $k_i$  the wave numbers for the neutron and proton, respectively,  $N_T^D$  and  $N_{\sigma T}^D$  are distortion factors,  $J_T$  and  $J_{\sigma T}$  are the volume integrals (for  $q = 0$ ) of the spin-independent  $(\tau_1 \cdot \tau_2)$  and spin-dependent  $(\sigma_1 \cdot \sigma_2 \tau_1 \cdot \tau_2)$  parts of the isovector central terms including the contribution from knockout exchange, and  $\langle F \rangle$  and  $\langle GT \rangle$  are Fermi and Gamow-Teller matrix elements. The latter are given by

$$\langle GT \rangle = (2J_i + 1)^{-1/2} \langle J_f || \sum_k t_-(k) \sigma(k) || J_i \rangle$$

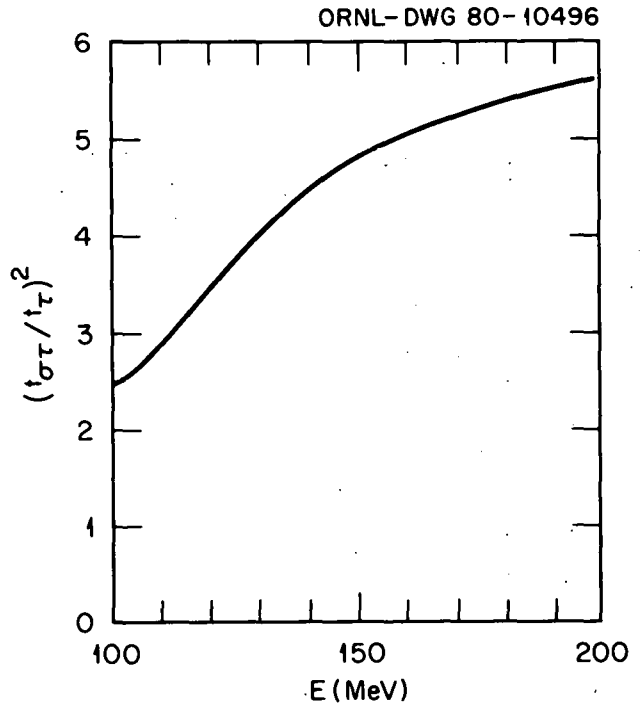
and

$$\langle F \rangle = (2J_i + 1)^{-1/2} \langle J_f || T_- || J_i \rangle.$$

Note that  $\langle GT \rangle$  has the same form as the spin dependent part of the isovector M1 operator. The distortion factors are given by the ratio of the calculated distorted-wave to plane-wave cross sections evaluated at  $\theta = 0^\circ$ .

Goodman et al.<sup>31)</sup> have measured zero degree cross sections at  $E_p = 120$  MeV for a number of light elements for which the Fermi and GT matrix elements were known from beta decay. From these data and calculated values for the corresponding distortion factors they deduced values for the volume integrals  $|J_T| = 89$  MeV-fm<sup>3</sup> and  $|J_{\sigma T}| = 168$  MeV-fm<sup>3</sup>. These agree within about 15% with the respective values calculated<sup>29)</sup> by Love. A further prediction of the calculations<sup>29)30)</sup> is that

$|J_{\sigma T}|$  remains relatively constant between  $E_p = 100$ –200 MeV (from reference 29).  $|J_T|$  decreases in value (see Fig. 12). This feature can be utilized to distinguish between  $\Delta S = 0$  and  $\Delta S = 1$  transitions.



A time-of-flight spectrum for the  $^{208}\text{Pb}(p,n)^{208}\text{Bi}$  reaction at  $E_p = 120$  MeV is shown in Fig. 13. The experimental energy resolution here is about 0.67 MeV. One can see a sharp peak sitting on top of a broad peak near 15 MeV. The sharp peak corresponds to the IAS of the  $^{208}\text{Pb}$  g.s., while the broader peak which lies about 0.4 MeV higher in excitation is the giant GT resonance. The peak labeled 7.5 MeV IAS is believed to correspond to the analogue of the M1 radiation identified at ORELA. This assignment is made on the basis of energetics as well as its cross section relative to that of the GT, which is comparable to the ratio of the squares of the CG coefficients for  $T = T_0$  and  $T = T_0 - 1$ . The peak labeled 9.2 MeV IAS(?) might correspond to the analogue of other M1 radiation in  $^{208}\text{Pb}$ . Figure 14 shows

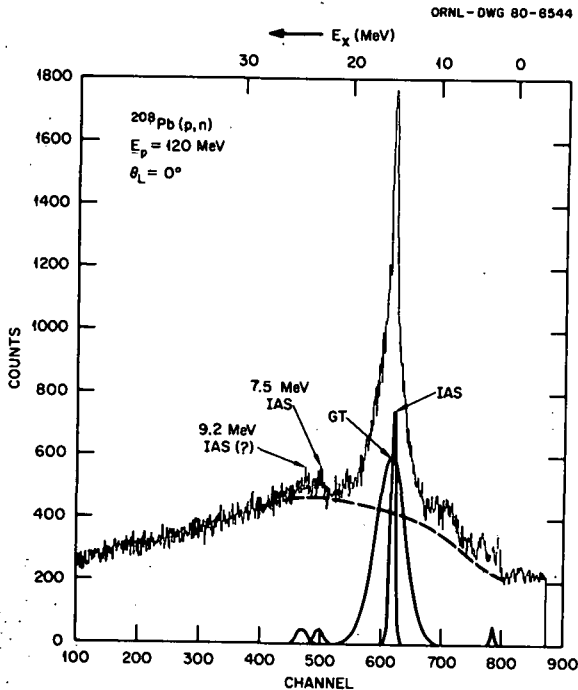


Fig. 13. Neutron time of flight spectrum for  $^{208}\text{Pb}(p,n)^{208}\text{Bi}$  reaction at  $E_p = 120$  MeV at  $\theta = 0^\circ$ .

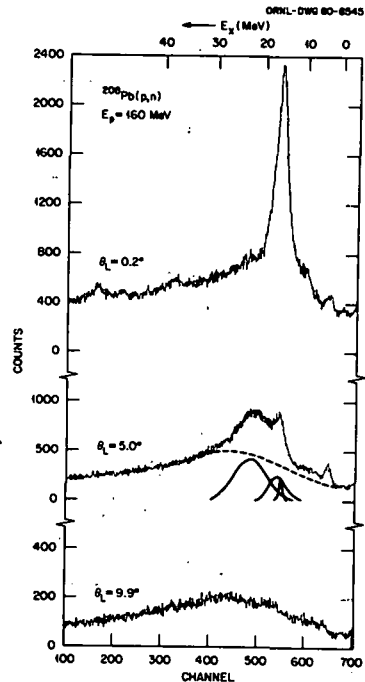


Fig. 14. Neutron time of flight spectra at  $\theta = 0.2^\circ$ ,  $5.0^\circ$  and  $9.9^\circ$  for  $^{208}\text{Pb}(p,n)^{208}\text{Bi}$  reaction at  $E_p = 160$  MeV.

spectra for the same reaction at 160 MeV. At this energy the cross section for exciting the GT relative to that for exciting the g.s. IAS is greatly enhanced. Our experimental enhancement is comparable (although somewhat smaller) than that predicted by Love.<sup>29)</sup> From our preliminary data it appears that the spin-independent potential does not decrease with increasing proton energy quite as rapidly as the calculations indicate. In the  $5.0^\circ$  spectrum one observes a new peak at  $E_x \sim 22$  MeV. This peak has an angular distribution similar to a peak at  $E_x = 2.8$  MeV. Figure 15 shows the differential cross sections for the g.s. IAS, GT and  $E_x = 2.8$  MeV resonances. The IAS and GT clearly involve  $\Delta l = 0$  and the latter  $\Delta l = 1$ . The 2.8 MeV resonance is identified as the  $h_{9/2}^{-1}13/2$  2- proton particle-neutron hole state previously suggested<sup>32)</sup> by Alford et al.

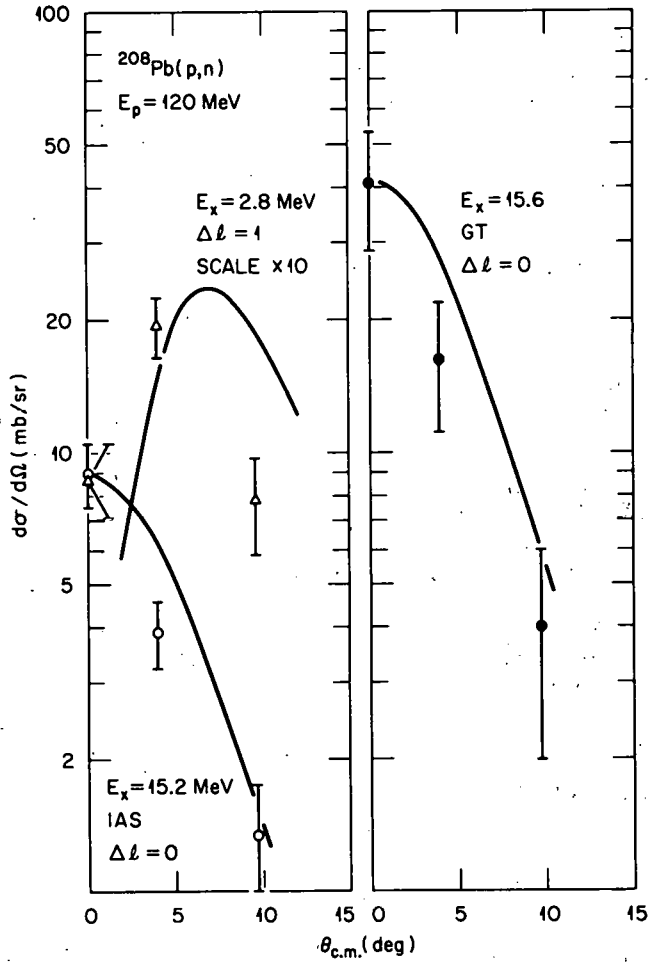


Fig. 15. Differential cross sections for the g.s. IAS, GT and  $E_x = 2.8 \text{ MeV}$  resonances for the  $^{208}\text{Pb}(p,n)^{208}\text{Bi}$  reaction at  $E_p = 120 \text{ MeV}$ .



Figure 16 shows spectra at a number of angles for the same reaction but at  $E_p = 200$  MeV. Here the g.s. IAS is completely dominated by the GT and it is not obvious that we will be able to extract its cross section at this energy. The  $\Delta l = 1$  resonance is clearly seen to peak about  $4.5^\circ$  beyond the GT. In  $^{90}\text{Zr}(p,n)$  at  $E_p = 120$  MeV, a  $\Delta l = 1$  resonance was observed<sup>33)</sup> at  $E_x = 17.9$  MeV. This is shown in Figs. 17 and 18. It has been suggested<sup>33)34)</sup> that these high lying  $\Delta l = 1$  resonances are the  $T = T_3$  members of a  $1^-$  isospin multiplet, of which the analogue of the GDR would be the  $T = T_3 + 1$  member. However,  $J = 0$  or  $2$  cannot be excluded. The cross section for excitation of this resonance in the  $^{208}\text{Pb}(p,n)$  reaction behaves similarly to that of the GT as a function of  $E_p$ , and thus has been identified<sup>34)</sup> as a  $\Delta l = 1$ ,  $\Delta S = 1$  transition. In  $^{208}\text{Bi}$ , e.g., this resonance can be thought to contain proton particle-neutron hole states of the type  $j_{15/2}i_{13/2}^{-1}$ ,  $i_{13/2}h_{11/2}^{-1}$ , etc. Recently data have been obtained at  $E_p = 200$  MeV for a series of targets ranging from lithium to lead. The  $\Delta l = 1$ ,  $\Delta S = 1$  resonance seems to be common to most targets.

Time-of-flight spectra at  $\theta = 4.3^\circ$  for  $^{90}\text{Zr}$ ,  $^{112}\text{Sn}$ ,  $^{124}\text{Sn}$ ,  $^{169}\text{Tm}$  and  $^{208}\text{Pb}$  are shown in Fig. 19. It is clear from this figure that the location of the  $\Delta l = 1$  peak occurs at nearly the same channel in the time of flight spectra for

each target which indicates the Q values are similar. If the interpretation of this resonance as a  $T = T_3$  member of a  $1^-$  multiplet (of which the analo-

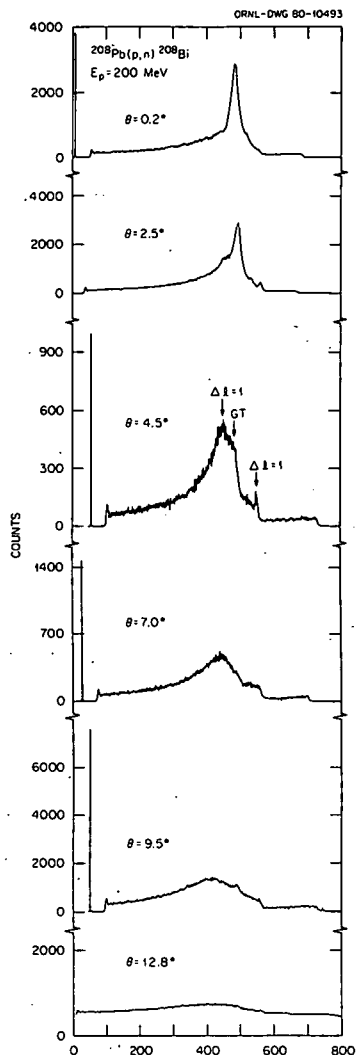


Fig. 16. Neutron time of flight spectra at  $\theta = 0.2^\circ$ ,  $2.5^\circ$ ,  $4.3^\circ$ ,  $7.0^\circ$ ,  $9.5^\circ$  and  $12.8^\circ$  for the  $^{208}\text{Pb}(p,n)^{208}\text{Bi}$  reaction at  $E_p = 200$  MeV.

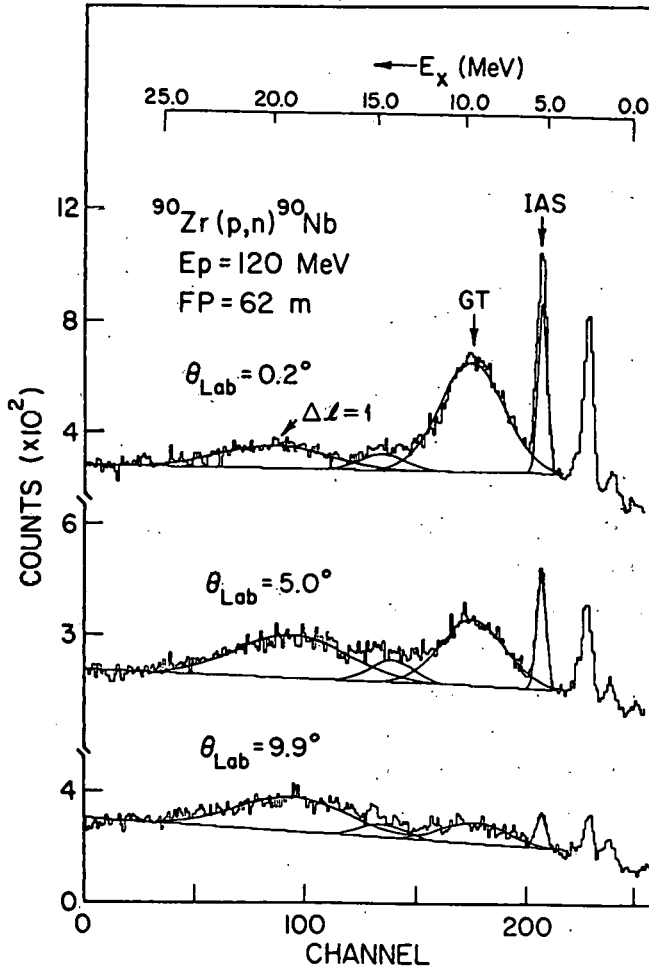


Fig. 17. Neutron time of flight spectra at  $\theta = 0.2^\circ$ ,  $5.0^\circ$  and  $9.9^\circ$  for the  $^{90}\text{Zr}(p,n)^{90}\text{Nb}$  reaction at  $E_p = 120 \text{ MeV}$ .

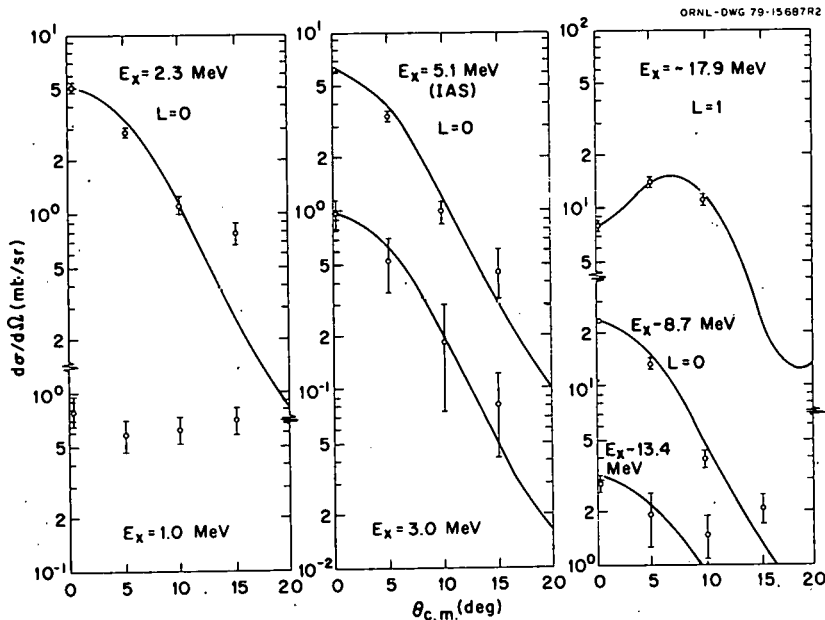


Fig. 18. Differential cross sections for resonances observed in the  $^{90}\text{Zr}(p,n)^{90}\text{Nb}$  reaction at  $E_p = 120$  MeV.

gue of the GDR is the  $T = T_3 + 1$  member is correct, one might expect the  $Q$ -values to be given approximately by

$$Q(1^-)_{T=T_3} \approx E_C + E_{\text{GDR}} - E_{\Delta T},$$

where  $E_C$  is the Coulomb displacement energy,  $E_{\text{GDR}}$  is the excitation energy of the GDR in the target nucleus, and  $E_{\Delta T}$  is the energy of the isospin splitting in the residual nucleus. One can use the isospin splittings found for  $^{90}\text{Zr}^{33)}$  and  $^{208}\text{Pb}^{34)}$  to find  $E_{\Delta T} \sim 40(N-Z)/A$  and show the above relationship to be approximately so. From the zirconium and lead data though, it appears that  $E_{\Delta T}$  is not linearly related to  $(N-Z)/A$ .

Ikeda et al.<sup>28)</sup> predicted that the energy difference between the giant GT resonance and the g.s. IAS would be approximately proportional to

$(N-Z)/A$ , where the proportionality factor is a function of angular momentum coupling coefficients, an average of radial matrix elements between neutron hole-proton particle states, and the strengths of the residual interactions in singlet and triplet spin states. There are also other simplifying assumptions involved, but they will not be detailed here. The same work is also applicable<sup>28)</sup> to a  $\Delta l = 1$ ,  $\Delta S = 1$  resonance for which the energy spacing from the g.s. IAS would also be approximately proportional to  $(N-Z)/A$ . Although the data are only in the preliminary state of analysis, the energy differences between the GT and  $\Delta l = 1$ ,  $\Delta S = 1$  resonances and the g.s. IAS are plotted against  $(N-Z)/A$  in Fig. 20. Both sets of data (with the exception of the  $^{90}\text{Nb}$  point for the  $\Delta l = 1$  resonance) seem to be described by straight lines which are nearly parallel. The GT data can be approximately fit by the relation

$$E_{\text{GT}} - E_{\text{IAS}} = -30.0(N-Z)/A + 6.7,$$

and the  $\Delta l = 1$  data by

$$E_{\Delta l=1} - E_{\text{IAS}} = -33.0(N-Z)/A + 13.6,$$

where the constants are in units of MeV. Now the coefficient of  $(N-Z)/A$  is basically what Ikeda et al. have calculated. In an extremely simplistic picture, it is just the energy separation between the singlet spin (e.g., the IAS with  $J^\pi = 0^+$ ,  $S = 0$ ) and triplet spin (e.g., GT with  $J^\pi = 1^+$ ,  $S = 1$ ) involving the

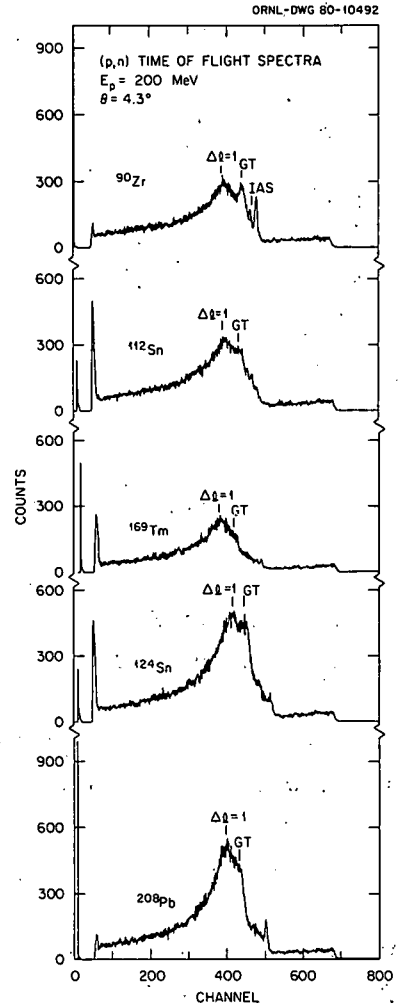


Fig. 19. Neutron time of flight spectra at  $4.3^\circ$  for the  $(p,n)$  reaction at  $E_p = 200$  MeV for targets of  $^{90}\text{Zr}$ ,  $^{112}\text{Sn}$ ,  $^{169}\text{Tm}$ ,  $^{124}\text{Sn}$  and  $^{208}\text{Pb}$ .

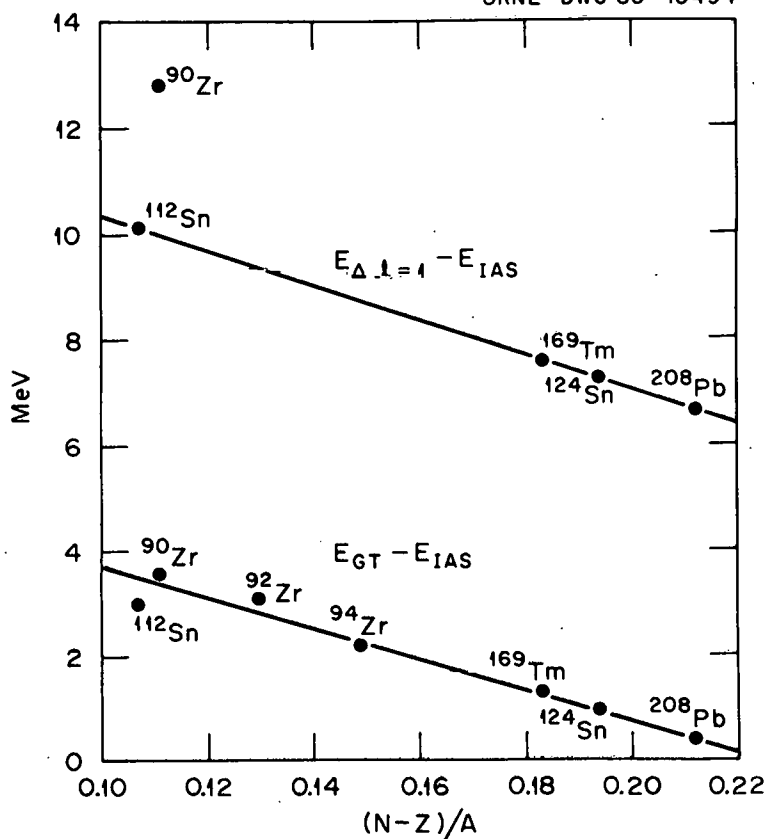


Fig. 20. Plots of  $(E_{GT} - E_{IAS})$  and  $(E_{\Delta l=1} - E_{IAS})$  versus  $(N-Z)/A$ . The data for  $^{92}, ^{94}\text{Zr}$  are from reference 36).

same  $\lambda_j$  as for the IAS) states without the effects of spin-orbit splitting. With the Rosenfeld admixture of  $v_s = 2/3 v_t$ , the work of Ikeda et al. would predict this coefficient to have the value  $(-30.7)$ . The value of the constant in the expression for  $E_{GT} - E_{IAS}$  would then be thought to represent an average spin-orbit energy. Similar comments can be made pertaining to the expression for  $E_{\Delta l=1} - E_{IAS}$ . Here, the constant also includes the energy splitting between  $\lambda$ -shells.

In Fig. 20, the  $E_{\Delta\ell=1} - E_{IAS}$  energy for the  $^{90}\text{Nb}$  is seen to be fairly high above the line. This also holds for the  $\Delta\ell=1$  resonances observed in  $^{92,94}\text{Nb}$ . This can probably be understood in terms of the shell model, where the number of particle-hole pairs which participate in the niobium isotopes is more limited and could have on average a higher energy splitting between  $\Delta\ell = 1$  shell states.

The question of the spin of this new  $\Delta\ell=1$ ,  $\Delta S=1$  resonance remains open. The most probable choices are  $1^-$  or  $2^-$ . A  $1^-(2^-)$  would suggest the existence of a collective E1 (M2) spin-flip type resonance. Both possibilities are interesting, and additional work is required both experimentally and theoretically to investigate the alternatives.

### Transition Strengths

The measured (p,n) cross sections also yield information concerning various transition strengths. It is usually assumed that the Fermi strength is exhausted in the g.s. isobaric analogue. The sum rule strengths for Fermi and GT transitions can be expressed as

$$S_{pn}(1) - S_{np}(1) = (N-Z),$$

and

$$S_{pn}(\sigma) - S_{np}(\sigma) = 3(N-Z),$$

respectively. Here,  $S_{pn}$  represents the sum over all final states of  $\langle GT \rangle^2$  (or  $\langle F \rangle^2$ ) for the (p,n) reaction, and  $S_{np}$  the analogous term for the inverse reaction (or  $\beta$ -decay). Nuclei with  $A > 90$  usually have large neutron excesses, and thus small values of  $S_{np}(\sigma)$  because the higher neutron shells are already filled. (This same condition is also responsible<sup>19)</sup> for causing the ohw M1 states in a target like lead to have mainly  $T = T_3$ .) Hence, one would expect  $S_{pn}(\sigma) \sim 3(N-Z)$  for such nuclei. For  $^{90}\text{Zr}(p,n)$  a value of  $\Sigma \langle GT \rangle^2 \sim 11$  has been found.<sup>33)</sup> The  $^{208}\text{Pb}$  data were analyzed by utilizing the values found for the volume integrals in reference 31) and  $\langle F \rangle^2 = 44$  to first determine  $N_T^D$ . Calculations indicate that  $N_T^D/N_{OT}^D \sim 0.8$ , and this relation was used to deduce  $N_{OT}^D = 0.059$ . Using this value of  $N_{OT}^D$  and  $|J_{\sigma\tau}|^2 = 168 \text{ MeV-fm}^3$ , the GT strength to the  $E_x = 15.6\text{-MeV}$  resonance in  $^{208}\text{Bi}$  was determined as  $\langle GT \rangle^2 \sim 48$ . Ikeda<sup>28)</sup> calculated that about 90% of the sum rule

strength should be located in a  $\langle GT \rangle$  resonance with a width of  $\sim 5$  MeV near the g.s. IAS. Our results are in reasonable agreement with those calculations, and seem to disagree with the suggestion<sup>35)</sup> that the GT strength should be highly fragmented in heavy nuclei. Almost all of the targets studied show a localized GT resonance (see, e.g., Fig. 19). Inclusion of the lower lying  $\Delta I = 0$  cross section and reduction of "assumed" backgrounds for the  $^{208}\text{Pb}(p,n)$  could raise the "observed" GT strength to about 65% of the limit. A final comparison of the fraction of GT strength observed must await further analysis of the abundance of data which now exists. It is important to resolve this question (because most of the strength goes to the  $T=T_0-1$  states) if one hopes to use the  $(p,n)$  reaction to deduce  $B(M1)$  values for the target nuclei. As previously noted, the  $(p,n)$  reaction basically is a measure of the isovector M1 strength. The relationship between an M1 transition to a level  $|f\rangle$  with  $(T, T_0)$  in the target nucleus and the GT transition to its isobaric analogue  $|f'\rangle = N_T T_- |f\rangle$  with  $(T, T_0-1)$  is given by

$$B(M1)_{i \rightarrow f} = 3/8\pi \langle GT \rangle_{i \rightarrow f'}^2 (\mu_N)^2 \mu_0^2 \left\{ \begin{matrix} T_0 \\ 2T_0+1 \end{matrix} \right.$$

for  $T' = T_0$  or  $T_0+1$ , respectively. If one uses the bare magnetic moments for the proton and neutron, the observed cross section for the suggested IAS of the M1 strength in  $^{208}\text{Pb}$  near 7.5 MeV would give  $B(M1)$  considerably larger than the  $2.6 \mu_0^2$  (i.e.  $\sim 19 \mu_0^2$ ) found in the ORELA work. (If one were to use a quenched magnetic moment of  $\sim 0.6$  nm, the sum of the M1 strengths for the 7.5- and 9.2-MeV resonances would just about exhaust the M1 sum rule.) There is as yet no justification for using such a relationship to extract  $B(M1)$  values from our  $(p,n)$  data, and the numbers above are only given to exhibit some of the problems and are not to be taken seriously. Much additional work is necessary in order to obtain a detailed understanding of the problems involved before one will be able to quantify with confidence the GT strengths deduced from the  $(p,n)$  data for medium to heavy mass targets.

Even though the data are not yet fully analyzed, it is already apparent that the  $(p,n)$  reaction at intermediate energies can be expected to yield a

wealth of new information. This will include the systematics (i.e., energy, width, strength) of the GT,  $\Delta l = 1$  spinflip and most likely other resonances, angular distributions, etc. From these one should be able to learn details of the effective nucleon-nucleon interaction, information pertaining to collective spin oscillations, microscopic nuclear wave functions, and perhaps electromagnetic strengths. Studies using deformed targets such as  $^{169}\text{Tm}$  will no doubt add other features. Hence, the future looks bright for the "new" technique as a means to solve "old" as well as new problems.

The author wishes to thank the large number of people who have contributed to this work. This includes collaborators involved in both the ORELA and IUCF experiments as well as the supporting staffs. Of course, without their collaboration and assistance this effort would not have been possible. Special thanks are due to Betty McHargue for her patience in typing this manuscript. This work was sponsored by the Division of Nuclear Sciences, U.S. Department of Energy, under contract No. W-7405-eng-26 with the Union Carbide Corporation.



1. See for example, S. W. Cierjacks, in Proceedings of the International Conference on the Interactions of Neutrons with Nuclei, Lowell, Massachusetts, 6-9 July 1976, edited by E. Sheldon, (ERDA Report No. CONF-760715-P2, National Technical Information Service, Springfield, Virginia) (1976) 383.
2. D. J. Horen, J. A. Harvey and N. W. Hill, Phys. Rev. C 20 (1979) 478.
3. G. F. Auchampaugh, Los Alamos Scientific Laboratory Report No. LA-5473-MS, 1974 (unpublished).
4. F. G. Perey (private communication, 1978).
5. W. E. Kinney (private communication, 1978).
6. A. M. Lane and R. G. Thomas, Rev. Mod. Phys. 30 (1958) 257.
7. J. M. Blatt and L. C. Biedenharn, Rev. Mod. Phys. 24 (1952) 258.
8. L. Medsker and H. E. Jackson, Phys. Rev. C9 (1974) 709.
9. J. A. Farrell, G. C. Kyker, Jr., E. G. Bilpuch and H. W. Newson, Phys. Lett. 17 (1965) 286.
10. W. P. Beres and M. Divadeenam, Phys. Rev. Lett. 25 (1970) 596. See also M. Divadeenam, W. B. Beres and H. W. Newson, Ann. Phys. (N.Y.) 80 (1973) 231.
11. D. J. Horen, J. A. Harvey and N. W. Hill, Phys. Rev. C18 (1978) 722.
12. M. R. Schmorak, Nuclear Data Sheets 22 (1977) 487.
13. See for example, B. Block and H. Feshbach, Ann. Phys. (N.Y.) 23 (1963) 47.
14. D. J. Horen, J. A. Harvey and N. W. Hill, Phys. Lett. 67B (1977) 268; Phys. Rev. Lett. 38 (1977) 1344.

15. D. J. Horen, G. F. Auchampaugh, J. A. Harvey and N. W. Hill, Phys. Lett. 79B (1978) 39.
16. R. J. Holt and H. E. Jackson, Phys. Rev. Lett. 36 (1976) 244.
17. R. J. Holt, R. M. Laszewski and H. E. Jackson, Phys. Rev. C 15 (1977) 827.
18. S. Raman, in Neutron Capture Gamma-Ray Spectroscopy, ed. by R. E. Chrien and W. R. Kane (Plenum Press, New York, 1979) 193.
19. D. J. Horen, in "Survey of Ground-State Magnetic Dipole Strength", Proceedings of the Giant Resonance Topical Conference, Oak Ridge, Tennessee (1979) (to be published).
20. R. E. Toohey and H. E. Jackson, Phys. Rev. C6 (1972) 1440.
21. R. J. Holt, H. E. Jackson, R. M. Laszewski and J. R. Specht, Phys. Rev. C20 (1979) 93.
22. M. Moreh, S. Shlomo and A. Wolf, Phys. Rev. C2 (1970) 1144.
23. S. Raman, R. S. Hicks, R. A. Lindgren, B. Parker and G. A. Peterson, BAPS 24 (1979) 845.
24. See for example, J. R. Huizenga and L. G. Moretto, Annu. Rev. Nucl. Sci. 22 (1972) 427.
25. C. D. Goodman, C. C. Foster, M. B. Greenfield, C. A. Goulding, D. A. Lind and J. Rapaport, IEEE Trans. Nucl. Sci. NS 26 (1979) 2248.
26. E. P. Wigner, Phys. Rev. 56 (1939) 519.
27. M. Kawai, T. Teraswa and K. Izumo, Prog. Theor. Phys. 27 (1962) 404; Nucl. Phys. 59 (1964) 289.
28. K. Ikeda, S. Fujii and J. I. Fujita, Phys. Lett. 3 (1963) 271; J. I.

- Fujita, S. Fujii and K. Ikeda, Phys. Rev. 133 (1964) B549; K. Ikeda, Prog. Theor. Phys. 31 (1964) 434; J. I. Fujita and K. Ikeda, Nucl. Phys. 67 (1964) 145.
29. W. G. Love, in the (p,n) and Nucleon-Nucleon Force, ed. by C. Goodman, S. M. Austin, S. D. Bloom, J. Rapaport and G. R. Satchler (Plenum Press, New York, 1980) 23; Contribution to LAMPF Workshop on Nuclear Structure Studies with Intermediate Energy Probes, Los Alamos, New Mexico (January, 1980).
  30. F. Petrovich, in the (p,n) Reaction and Nucleon-Nucleon Force, op. cit. 115.
  31. C. D. Goodman, C. A. Goulding, M. B. Greenfield, J. Rapaport, D. E. Bainum, C. C. Foster, W. G. Love and F. Petrovich, preprint (September, 1979).
  32. W. P. Alford, J. P. Schiffer and J. J. Schwatz, Phys. Rev. C3 (1971) 860.
  33. D. Bainum, J. Rapaport, C. D. Goodman, D. J. Horen, C. C. Foster, M. B. Greenfield and C. A. Goulding, preprint (September 1979).
  34. D. J. Horen, C. D. Goodman, C. C. Foster, C. A. Goulding, M. B. Greenfield, J. Rapaport, D. E. Bainum, E. Sugarbaker, T. G. Masterson, F. Petrovich and W. G. Love, preprint (February, 1980).
  35. G. E. Brown, J. S. Dehesa and J. Speth, Nucl. Phys. A330 (1979) 290.
  36. W. Sterrenberg, S. M. Austin, D. E. Bainum, R. P. DeVito, C. C. Foster, A. Galonsky, C. D. Goodman, C. A. Goulding, M. B. Greenfield, D. J. Horen, J. Rapaport and E. Sugarbaker, Contribution to Conference on Extreme States in Nuclear Systems, Dresden, W. Germany (February, 1980).